Emergence EEG pattern classification in sevoflurane anesthesia

To cite this article before publication: Zhenhu Liang *et al* 2018 *Physiol. Meas.* in press https://doi.org/10.1088/1361-6579/aab4d0

Emergence EEG pattern classification in sevoflurane anesthesia

Authors: Zhenhu Liang[1], Cheng Huang[1]， Yongwang Li[2], Darren F. Hight[3], Logan J. Voss[3], Jamie W. Sleigh[3], Xiaoli Li [4] , Yang Bai[5*]

Affiliations:

[1] Institute of Electrical Engineering, Yanshan University, Qinhuangdao, China

[2] The General Hospital of the PLA Rocket Force, Beijing China

[3] Department of anesthesia, Waikato Hospital, Hamilton, New Zealand

[4] State Key Laboratory of Cognitive Neuroscience and Learning & IDG/McGovern Institute for Brain Research, Beijing Normal University, Beijing, China

[5] International Vegetative State and Consciousness Science Institute, Hangzhou Normal University, Hangzhou, Zhejiang, China

Correspondence to: Dr. Yang Bai. Email: baiyang1126@gmail.com

Interest disclosure: The authors declare no conflict of interest.

Highlights:

► Four emergence EEG patterns were found in γ-amino-butyric acid (GABA)-ergic anesthetic drugs.

► Genetic algorithm combined with support vector machine (GA-SVM) was proposed to identify the emergence EEG patterns.

► The relative power spectrum density (RPSD) was used as the feature to classify emergence EEG patterns and got a good accuracy.

►The statistics shows that the emergence EEG patterns are age-related and may have value in assessing postoperative brain states.

Abstract:

Objective. Significant spectral characteristics of electroencephalogram (EEG) patterns exist in individual patients during re-establishing consciousness after general anesthesia. However, these EEG patterns cannot be quantitatively identified using commercially available depth of anesthesia (DoA) monitors. This study proposed an effective classification method and indices to classify these patterns among patients.

Approach. Four types of emergence EEG patterns were identified based on EEG data set from 52patients undergoing sevoflurane general anesthesia from two hospitals. Then, the relative power spectrum density (RPSD) of five frequency sub-bands of clinical interest (delta, theta, alpha, beta, and gamma) were selected for emergence state analysis. Finally, the genetic algorithm support vector machine (GA–SVM) was used to identify the emergence EEG patterns. Performance was reported in terms of sensitivity (SE), specificity (SP) and accuracy (AC).

Main results. The combination of the mean and mode of RPSD in delta and alpha band (P (delta)/P (alpha) performed the best with the GA-SVM classification. AC indices obtained by GA-SVM across the four patterns were 90.64 ± 7.61, 81.79 ± 5.84, 82.14 ± 7.99, and 72.86 ± 11.11 respectively. Furthermore, the emergence time of the patients with EEG emergence pattern I and III increased with the increasing of patients' age. While for the patients with EEG emergence pattern IV, the emergence time positively correlates with the patients' age which less than 50, and negatively correlates with the patients' age which more than 50.

Significance. The mean and mode of P (delta)/P (alpha) is a useful index to classify the different emergence EEG patterns. In addition, the EEG emergence patterns may correlate with underlying neural substrate which related with patients' age.

1. Introduction

How the brain transitions between conscious and unconsciousness states in the brain remains a pending question in neuroscience (Purdon et al., 2013b). To better understand the general anesthesia mechanism and to develop more sophisticated intraoperative neurophysiologic monitoring techniques, an investigation on the nature of the anesthetic induction and emergence process (the exit from the anesthetized state) is urgently needed.

Electroencephalogram (EEG) has been widely applied in exploring the neurological changes in individuals during anesthesia (Rampil, 1998;Jameson and Sloan, 2006). The commonly used gamma-amino-butyric acid-ergic (GABAergic) anesthetic drugs have several different effects on EEG measurements. For example, early loss of consciousness is associated with loss of power in the high frequency range and a strong "biphasic" rise in total power (Bojak and Liley, 2005) associated with diffuse β-rhythms. A surgical level of general anesthesia is associated with α-rhythms and slow activity (delta rhythms) (McCarthy et al., 2008;Ching et al., 2010), while deeper anesthesia induces a state where the EEG periodically switches between "burst" and "suppression" periods ("burst suppression"). After the anesthetic withdrawal, delta and/or alpha waves disappear and beta (15–30Hz) waves appear instead before waking.

Recently several research groups have attempted to characterize the emergence EEG patterns and to analyze the underlying mechanism of the emergence process to enhance post-surgical recovery. For example, Breshears et al. analyzed the electrical activity of electrocorticography (ECoG) during both the induction and the emergence processes in propofol anesthesia(Breshears et al., 2010). They found that slow oscillation (<0.5 Hz) in large-scale functional networks are maintained during the

loss of consciousness (LoC) and recovery of consciousness (RoC) processes. In addition, theta and gamma phase–power coupling occurs throughout the induction and emergence process. Law et al. found that many patients experienced different levels of pain and nausea during emergence (Law et al., 2011). Furthermore, several studies pointed out that the emergence process does not mirror the induction process. In other words, the RoC process has a distinct neurobiological mechanism(Kelz et al., 2008;Law et al., 2011). Purdon et al. recorded high-density EEGs during gradual induction and emergence from unconsciousness after anesthesia with propofol. The low-frequency EEG power (<1Hz) and the occipital alpha oscillations (8–12 Hz) were found to decrease after RoC (Purdon et al., 2013b). Lee et al. proposed that both continuous and discrete modes existed during LoC and RoC processes (Lee et al., 2011). Hight et al. analyzed the clinical EEG recordings and used Bayesian methods to estimate the likelihood of an EEG pattern corresponding to the position of the patient on a 2D manifold in a state space of excitatory connection strength (Hight et al., 2014).

None of the current depth of anesthesia (DoA) monitors or DoA indices derived from the prefrontal EEG provide identification of the different emergence EEG patterns. These measures and indices include the bispectral index (BIS) monitor (Aspect Medical Systems, Newton, MA, USA) (Rampil, 1998), M-entropy module (GE Healthcare, Helsinki, Finland) (Viertiö‐Oja et al., 2004), permutation entropy (PE) (Li et al., 2008), approximate entropy (ApEn) (Bruhn et al., 2000), and detrended fluctuation analysis (DFA) (Jospin et al., 2007) etc. It is noteworthy that Hight, et al. found that different emergence EEG patterns apparently exhibit different power spectrum characteristics (Hight et al., 2014). They categorized the wake-up period into two patterns, namely, archetypal emergences and non-archetypal emergences, based on the spectral characteristics. However, in this paper, we found four emergence EEG patterns. Classification method based on power spectrum

density can be used to identify emergence EEG patterns and to analyze their possible neurophysiological differences.

A single parameter is inadequate to classify the multiple states during the time evolution of the emergence period. The methods for feature extraction are usually combined with the classification methods to solve this problem (Shalbaf et al., 2013;Chen et al., 2014;Riaz et al., 2015). In this study, considering the imbalanced distribution of the biological samples, SVM was used for emergence EEG pattern classification. The SVM is a typical classification method and it exhibits well performance in a small sample, nonlinear and high-dimensional classifications compared with KNN(K-Nearest Neighbour), ANN(Artificial Neural Networks) and Random Forest (Cover and Hart, 1967;Mckeown, 1993;Hsu and Lin, 2002;Lin, 2003). In addition, the relative power spectrum density (RPSD) (Bian et al., 2014) within different frequency bands were considered as the EEG features to classify the four emergence patterns

The remainder of this paper is organized as the follows: Section 2 presents the EEG recording and EEG preprocessing. In Section 3, the feature extraction and classification methods, as well as the performance evaluation are described in detail. The different recovery trajectories after anesthesia and the classification results are presented in Section 4. Finally, the discussion and conclusion are given in Section 5.

2. Materials and emergence EEG patterns

2.1 EEG recordings

In this study, two EEG data sets were used for analysis. The details of them are described below:

(A) EEG data set I

Raw EEG signals were recorded from 44 patients (24 females and 20 males), aged 21–71 years. American Society of Anesthesiologists (ASA) physical status I or II were enrolled in this study from the general hospital of the PLA rocket force in Beijing, China. Approval from the general hospital of the PLA rocket force was obtained, and all the subjects provided their informed consent.

About 2 mg/kg of Midazolam and 5 μg/kg of Sufentainil were administered after the patients entered the operating room. Then anesthesia was induced through intravenous injection with 2 mg/kg of midazolam, 5 μg/kg of sufentainil, 80 ug/kg of remifentanil, and 14 mg/kg of cisatracurium. Remifentanil was administered intravenously, and sevoflurane was administered via a vaporizer; these drugs were combined to maintain the general anesthesia. Time of LoC was determined every 5s by loss of response to a verbal command, and the time of RoC was determined by the time that the patient first responded to a verbal command.

Front-temporal EEGs were recorded using the Bio-Acquisition Systems (Bio-AMP8, Kangpu Medical, Huzhou, Zhejiang). The bipolar montage (Fp1–Fpz) was used to collect the EEG recordings according to the international 10-20system, and Fpz was used as the ground electrode. Impedance was maintained at <5 kΩ. The sample rate was 1 kHz.

(B) EEG data set II

Eight patients (5 females and 3 males) aged 21–88 with ASA physical status between I and III were recruited from the Waikato District Health Board Hospital in Hamilton, New Zealand. All of the participants provided their informed consent and the study was approved by the New Zealand Health and Disability Ethics Committee.

Anesthesia was induced with 1.5–2mg/kg of propofol and 4 μ g/kg of Fentanyl, injected intravenously. Then, sevoflurance was used for maintenance. The time of RoC was counted as the

moment the patient spontaneously opened their eyes for more than 5s, or could respond to the command "open your eyes."

EEG signals were recorded using the BIS (Aspect Medical System, Newton, MA, USA), the BIS monitor utilized a standard EEG montage in clinic, where the silver-silver chloride strip sensor was placed at the position approximately to Fpz and Fp1/2 leads of 10-20 standard EEG montage, and electrode-skin impedance was maintained at <7.5 kΩ, the sample rate of the EEG was 128 Hz. For the BIS utilized the referential montage, two EEG recordings can be achieved (Fpz-F7 and F1-F7). In this study, we analyzed the EEG recording of F1-F7.

2.2 EEG preprocessing

The same preprocessing method was used for these two datasets. Firstly a band-stop IIR filter (49–51Hz) was used to cancel the main noise of 50 Hz, and the outliers were eliminated (larger than 200μV). Then the EEGLAB function *eegfilt.m* was used to remove the frequency band of 0–0.5Hz. Next, the electromyography (EMG) and other high-amplitude transient artifacts were removed with an inverse filter (Schlögl, 2000;François et al., 2007). Finally, all these two datasets were down sampled to the same frequency of 100 Hz using the Matlab function of *resample.m*.

3. Methods

3.1 Feature extraction

Relative power spectrum density

The EEG oscillation is mainly divided into five sub-bands based on the clinical interest: delta (0–4Hz), theta (4–8Hz), alpha (8–13Hz), beta (13–30Hz), and gamma waves (30–47Hz) (Proakis et al., 1992). For these sub-bands, the power spectral density (PSD) was computed using the *pwelch* method (Welch, 1967). Then the RPSD is given by:

$$RPSD(f1, f2) = \frac{p(f1, f2)}{p(1,47)} \times 100\% \quad (1)$$

where $p(\cdot)$ indicates the power, and $RPSD(\cdot)$ is the relative power spectral density, and f_1 and f_2 are the low and high frequency, respectively. The $P(1,47)$ is the power from 1Hz to 47 Hz , and it includes all five sub-bands (delta, theta, alpha, beta, and gamma) (Buzsáki and Draguhn, 2004). Therefore, five types of RPSD with bands/sum were obtained. In addition the 10 ratios (P(delta)/P(theta) [or/P(alpha), or/P(beta), or/P(gamma)], P(theta)/P(alpha) [or/P(beta), or/P(gamma)], P(alpha)/P(beta) or /P(gamma), P(beta)/P(gamma)) of RPSD with power among different frequency bands were computed for possible pairs of frequency bands expressed as follows

$$RPSD(\frac{band1}{band2}) = \frac{p(band1)}{p(band2)} \times 100\% \quad (2)$$

All the RPSD values were computed at that: the EEG data samples of 10 s were divided into overlapping segments with 50% overlap.

In summary, there are 15 variations of RPSD—for each of EEG signals of 52 subjects were extracted. For all the indices were calculated with the epoch of 10s and 50% overlap. The emergence is a time course, which usually sustain more than 10 minutes. So, we can achieve more than 200 values for one emergence index in one patient. Considered the variation of the indices with time, the statistics of the mean, median, mode, maximum(max), minimum(min), and standard deviation (SD) of the indices in a time window of 1.5 minutes (about 24 values) were calculated to eliminate the effects of the noise. In order to achieve the best classification feature, the combination of different statistical methods with one index and different statistical methods with different index were employed as the classifier features. Combining the type of indices and statistics methods, we can achieve more than 100 features. If we assembling two –paired features for classification, the number

of the combinations will be more than 5,000. The three or more features' combinations will be a huge number. So, in this study, we mainly considered to use the 15 indices with two statistical indicators as the classification features. For comparison, we calculated six combinations: group #1(mean, SD), group #2(mean, mode), group #3(median, mode), group #4(mean, mode, min, max, median, SD), group #5(minimum, mode) and group #6(mean, mode, SD), respectively.

3.2 Genetic algorithm–support vector machine (GA–SVM)

In this study, we adopt a classical classification method which combine the LIBSVM and Genetic algorithm, called GA-SVM. The LIBSVM developed by Chih-jen Lin supports multi-class classification with the "one-against-one" approach, in which $k \times (k-1)/2$ classifiers are constructed and each one train data from two different classes(Chang and Lin, 2011).

The SVM is a well-established classification technique (Boser et al., 1992;Cortes and Vapnik, 1995). Given a training set of instance-label pairs (x_i, y_i), where $x_i \in R^n$, $y \in \{1,-1\}^l$, $i=1,....l$. The SVM is well known for creating a separating hyperplane with a maximal margin. The optimal hyperplane can be obtained by solving the following optimization problem:

$$\min_{w,b,\xi} \frac{1}{2} w^T w + c\sum_{i=1}^{l} \xi_i \tag{3}$$

$$\text{subject to} \quad y_i(w^T \phi(x_i) + b) \geq 1 - \xi_i \tag{4}$$

$$\xi_i \geq 0, i = 1, \ldots, l,$$

where (3) is the convex cost function, (4) is the constraints, the optimal w, the vector variable is determined with a dual problem and the primal-dual relationship and $c > 0$ is the penalty factor for misclassified points(Cortes and Vapnik, 1995). The decision function is:

$$\text{sgn}(w^T \phi(x) + b) = \text{sgn}(\sum_{i=1}^{l} y_i a_i K(x_i, x) + b) \tag{5}$$

where $\mathrm{sgn}(\cdot)$ is the sign function, which is used for extracting the sign (positive or negative) of a real number. $K(x_i, x_j)$ represents kernel function that is mapped into high-dimensional space. The nonlinear separating hyperplane can be found by constructing a Lagrangian multiplier method, the equation of which is as follows:

$$\min Q(\alpha) = \frac{1}{2}\sum_{i=1}^{N}\sum_{i=1}^{N} y_i y_j \alpha_i \alpha_j K(x_i, x_j) - \sum_{i=1}^{N} \alpha_i \tag{6}$$

subject to $$\sum_{i=1}^{N} y_i \alpha_i = 0, \quad 0 \le \alpha_i \le C, \quad i = 1,2,...,N \tag{7}$$

where $\alpha = (\alpha_1,...,\alpha_N)$ is the vector of the nonnegative Lagrange multipliers that meet he constraints in (3). Some kernel functions have been proposed in the literature(Huang and Wang, 2006;Martino et al., 2011a),which were shown as (8),(9),(10).

Polynomial kernel:

$$K(x_i, x_j) = (1 + x_i \cdot x_j)^d \tag{8}$$

Radial basis function kernel:

$$K(x_i, x_j) = \exp(-\gamma \left\| x_i - x_j \right\|^2) \tag{9}$$

Sigmoid kernel:

$$K(x_i, x_j) = \tanh(k x_i \cdot x_j - \delta) \tag{10}$$

In this study, RBF could handle the relationship between class labels and attributes (Hsu et al., 2003;Lin, 2003). When SVM is used with the RBF kernel, the parameters C and γ is must be set, C is the penalty factor for misclassified point. If C is too large, a higher penalty for non-separable points is added, thus leading to store too many support vectors and possibly resulting in over fit. On the other hand, if C is too small, an under fitting can occur. The γ parameter specifies the radius of the RBF, which has an effect on the accuracy(Huang and Wang, 2006).

Genetic algorithms(GA) are adaptive heuristic search algorithms inspired by the theory of natural evolution and it simulate the evolution of species to solve the optimization problem. In this study, we applied GA into SVM to search for the best parameters C and γ. In the GA algorithm, we defined the parameters C and γ of SVM as genetic representation, and the classification accuracy was defined as the fitness. Then we initialized a sample including 20 possible solutions randomly selected from -25 to 25. The inheritance rate was 0.2, the crossover rate was 0.7 and the mutation was 0.1.

The classification of the GA-SVM process is briefly described as follows:

(i) Data pre-processing was performed firstly by randomly dividing these features, relative power spectrum density (RPSD) of five EEG sub-bands power, into two datasets: testing sets (20% of all datasets) and train sets (80% of all datasets). Each sample was labeled as one of the four emergence EEG patterns according to an anesthetist's judgment.

(ii) The MATLAB function *mapminmax.m* was used to normalize the vector to represent the features in the range of $[-1,+1]$.

(iii) We took an RBF kernel, the best parameters (C and γ) of which were searched on the basis of the GA.

(iv)The classification model was trained by train sets based on LIBSVM tools and the classification results were obtained.

In this study, in order to assess the performance of GA-SVM, we compared the classification methods of grid-search based SVM (GS-SVM), the BP neural network and the random forest. The detailed description of these machine learning methods and performance comparison are shown in Appendix.

3.3 Performance evaluation

The performances of GA-SVM were evaluated in terms of sensitivity (SE), accuracy (AC), and specificity (SP), respectively, more details can be found in previous studies (Fraiwan et al., 2012). The calculations are defined as follows:

$$SE = \frac{TP}{TP + FN} \tag{11}$$

$$AC = \frac{TN + TP}{TN + TP + FP + FN} \tag{12}$$

$$SP = \frac{TN}{TP + FN} \tag{13}$$

where the TP, TN, FP and FN are the numbers of the true positives, true negatives, false positives and false negatives, respectively.

4. Results

Following the end of surgery after anesthetic administration is stopped, the most notable feature is the loss of alpha activity and increase in beta power. However, the EEG patterns during emergence are not always identical (Hight et al., 2014). In this study, we found four typical EEG patterns during emergence period.

Pattern I: Alpha loss, delta persistent

Pattern I is characterized as alpha loss and delta persistent. A complete EEG recording of pattern I (from data set I) is illustrated in Figure 1. Figure 1(A) marks the detailed anesthetic process. Where, from (e) to (j) is marked as the emergence period. Figure 1(B) and (C) are the preprocessed EEG recordings and the corresponding spectrogram. It can be seen that at the start of emergence period, the power of alpha suddenly disappeared, and the delta waves increased in power.

"Figure 1 around here."

Pattern II: Alpha and delta wave loss

Figure 2 displays the EEG characteristic of pattern II (from data set II) with both alpha and delta wave losses during the emergence state. The preprocessed EEG recording is shown in Figure 2(A). The corresponding spectrogram shown in Figure 2(B) has clear alpha and delta power in the moderate anesthesia state. Following the start of emergence, the frequency of alpha power centered at 12 Hz disappeared, and at the same time the power of delta significantly decreased. Then all frequency bands of signal can be seen at the end of emergence.

"Figure 2 around here."

Pattern III: Alpha and delta persistent

Pattern III (from data set I) shows persistence in both the alpha and delta bands after surgery. As shown in Figure3, the spectrogram exhibited the strong alpha and delta power whether in anesthesia or in emergence state. The waveform with broadband power appears at 1000 s and continuing until patient response.

"Figure 3 around here."

Pattern IV: Only delta persistent

Pattern IV (from data set I) is a non-archetypal emergence pattern. As shown in Figure 4, the spectrogram of the EEG presented almost no changes. Only the delta frequency band was seen, and there was a complete absence of alpha activity throughout the EEG recording.

"Figure 4 around here."

The framework for the classification of the emergence EEG patterns was shown in Figure 5. First, the EEG datasets and emergence EEG patterns were collected, and the emergence state data was extracted on the basis of the event recording. Each sample was labeled as one of the four emergence EEG patterns based on the frequency spectrum features. Then, the 15 variations of RPSD

for each frequency band with the statistics indices of the mean, median, mode, max, min, and SD were calculated and used as the classification features. The samples were randomly divided into the training and testing sets, in which 80% of the samples were used for training and 20% for testing. Finally, the SE, AC and SP were used for the classification performance evaluation.

"Figure 5 around here."

Considering the inadequacy of the existing methods and the significant differences in the spectrograms among the different emergence patterns, the GA–SVM based on the 15 RPSD variants were used to classify the four emergence patterns. The cross-validation accuracy of the 15 indices under each statistical indicator is shown in Figure 6. The indices of RPSD(delta/alpha) were higher than the other indices. Table 1 presents more detailed information concerning the accuracy statistics of RPSD(delta/alpha) for Training set and Testing set with several typical combinations of indicator, In the Table 1, the group numbers denote the typical combinations of statistics indices and used as the classification features. It can be observed that the group #2 had the highest testing accuracy(75.48 ±10.75) among all six groups. Thus, the mean and mode of indices of P (delta)/P (alpha) (statistical indicators of group #2) were taken as the best classification features to classify the emergence patterns. Next, the classification performance of GA-SVM was evaluated based on the statistics indices of AC, SE and SP. The related statistics of each classification were shown in Table 2. It can be observed the GA-SVM excited a high AC and SP.

"Figure 6 around here."

"Table 1 around here."

"Table 2 around here."

We believe that classification based on the multi-feature can bring high predictive accuracy.

However, considered the issues of the real time and complexity on the clinical application. We prefer to utilize less feature to achieve high prediction accuracy. Based on the result of figure 6, it can be see that the classification features of the combine of delta/alpha's mean and mode (group #2) had the best prediction accuracy in all features that we calculated. Also, it seems that the alpha/beta and alpha/gamma had relative high prediction accuracy. So, we considered to employ the alpha/beta, alpha/gamma and delta/alpha as the classification features. The predictive accuracy values of this combination in six groups are 61.04%, 61.78%, 59.58%, 61.67%, 59.06%, and 63.02%, respectively. It can be seen that these predictive accuracy values are very low compared with the combination of the delta/alpha's mean and mode. What's more, it consume more than 30 minutes for training and testing.

Furthermore, to analyze the potential inner relationship between emergence EEG patterns and physiological information, we collected statistics for all the class subjects classified and shown in the Table 3. According to the spectrum characteristics of these four classifications during the anesthesia maintenance stage, the groups of patterns (patterns I-III) showed the archetypal anesthesia, which consists of the frequency of alpha and delta. Pattern IV was considered as the non-archetypal anesthesia, which included only the frequency of delta. Moreover, age was closely related to the pattern of the archetypal anesthesia emergence period, while the non-archetypal anesthesia presents different relationship between the emergence time and patients' age. The variables of patient gender, anesthesia drug type, and duration of recovery had no statistically significant effect in these four patterns. Due to a small number of pattern Ⅱ, furthermore, the relationship between patients' age and the duration of recovery process for archetypal anesthesia(pattern I and III) and non-archetypal anesthesia was analyzed. As shown in Figure 7, for the pattern I and pattern III with the increasing

age, the time required to emergence period from sedation also increased. Older people seemed to need more time to wake up from anesthesia. As shown in Figure 8, there appears to be the same relationship between patients' age and the emergence time for the patients with EEG emergence pattern Ⅳ in the cases where the patients' age is less than 50. However, with the increasing age, the emergence time was decreased for the patients' age more than 50. Middle-aged individuals required more time to wake up.

"Table 3 around here."

"Figure 7 around here."

"Figure 8 around here."

5. Discussion and conclusion

The mechanism of loss and recovery of consciousness under anesthesia still remains unclear. The variation in EEG patterns exhibited during emergence from anesthesia makes DoA monitoring a research challenge.

In this study, four emergence EEG patterns were found in all EEG recordings, and the SVM combined with EEG derived features were employed for analyzing anesthetic EEG recordings to classify the emergence trajectories. The results showed that three archetypal anesthesia patterns and one non- archetypal anesthesia patterns were found in four emergence EEG patterns. In all classification features, the P (delta)/P (alpha) index exhibited better performance than the other RPSD indices. What's more, in order to verify the performance of GA-SVM, we compared it with BP neural network, GS-SVM and Random Forest. The performance of different classification methods were also evaluated by the SE, AC and SP. The results showed that GA-SVM has a better performance than other three machine learning methods. The following are the interesting findings

on and advantages of the GA–SVM classification based on RPSD:

(i) The features are extracted from the frequency sub-band to avoid the unreliable features of original signal, which varies significantly with individuals, different activities of the human body and other uncontrollable variables.

(ii) A multi-class classification can be achieved in admitting more potential emergence EEG patterns.

(iii) A potential relationship is found between age and the emergence time in the archetypal anesthesia and non-archetypal anesthesia.

Different emergence processes may be related to different arousal mechanisms and may provide important insights into the postoperative cognitive dysfunction. Although Hight et al.(Hight et al., 2014) attempted to use a sleep-manifold model to describe the mechanisms, the patterns were not categorized in detail and the clinical applications were not considered. Lee et al. analyzed the EEG recording of volunteers and classified the anesthesia into two patterns of groups based on the connection strength on information transmission with multi-channel EEG (Lee et al., 2011). The merit of this study is that the analysis based on the clinical EEG data and the indices is simple in principle, yet applicable in practice. Further, Purdon et al. and Akeju et al. showed that EEG power across all frequency bands presented significantly age-related changes in the EEG spectrum and coherence during anesthesia(Akeju et al., 2015;Purdon et al., 2015). Similarly, we found that EEG dynamics varied significantly as a function of age during the emergence period and that elderly patients needed more time to recover. However, the commercial EEG-based DoA indices do not account for age and therefore are likely to be inaccurate in elderly patients or children. In this study, two data sets were recorded from different frontal area. Most of the researches showed that the frontal EEG has similar spectrogram features during anesthesia (Antkowiak, 1999;Murphy et al.,

2011;Purdon et al., 2013a). So, we speculated that the two data sets will not be affected by the recording positions. Therefore, the method proposed in this study could be used to improve brain state monitoring for different age groups, especially in the context of postoperative emergence.

However, this study involved only the classification of the emergence EEG patterns. There are still some issues that require further research. Firstly, several studies suggested that the EEG pattern under anesthesia occurs on a temporal as well as a spatial scale(Bettinardi et al., 2015;Trafidło et al., 2015). In addition, the anatomy and the physiology of the brain changes with ages, which may cause variable hemodynamic and neuronal responses(Fabiani et al., 2014). Therefore, the emergence EEG patterns on the spatial scale and cerebral metabolic change should be considered in further studies. Secondly, the influencing factors that could generate the different patterns should be more deeply explored. The statistics in our study demonstrated that the patient age could be an important factor in forming different patterns. However, we only considered the EEG in the frontal area and the number of samples is only 52; the lack of sample information made drawing a conclusion impossible. Especially there are only 4 samples in pattern II because of the limitation of data sets. Although the pattern II is rare to emerge in the patients during ROC, we believe that it may has more subjects for pattern II in a larger data sets. In the further study we will extend the sample size to investigate the underlying mechanisms for anesthesia induced diverse emergency patterns. Finally, multimodal analysis, such as EEG-fMRI or functional near-Infrared spectroscopy (fNIRS) should be used as a tool for deeper analysis(Franceschini et al., 2010). Lastly, from the perspective of pharmacokinetic-pharmacodynamic (PKPD) perspective, a delay effect occurs at the brain site after the cessation of anesthetic delivery. The anesthetic mechanism of emergence needs to consider the individualized metabolism difference.

In conclusion, this study researched the differences of EEG patterns in emergence processes among patients and then provided a classification method to distinguish different emergence EEG patterns. The patterns categorized can be used as a feature for understanding consciousness recovery. The GA–SVM method based on P (delta)/P (alpha) has a potential value in DoA monitoring. An in-depth study of these issues is vital to meaningful for the understanding of the mechanisms of anesthesia and DoA monitoring.

Acknowledgements

This research was supported by National Natural Science Foundation of China (61673333，61603327), Research project of Education department of Hebei province (GCC2014019) and Natural Science Fund for Excellent Young Scholars of Hebei Province of China (F2018203281).

Appendix A: The algorithm of GS-SVM, BP-NN and Random Forest.

(A) Grid search algorithm based SVM

The Grid search algorithm based SVM(GS-SVM) is an alternative method to find the best parameter of C and γ (Huang and Wang, 2006). This algorithm is simple and straightforward. This method just needs to set the grid range and search interval to get the best accuracy. Compared with the GA-SVM, the GS-SVM is time consuming.

(B) Back Propagation (BP) neural network

The Back Propagation neural network(BP-NN) algorithm was firstly proposed by Rumelhart and MaCelland and it is one of the most widely used neural network model(Li et al., 2012). The main characteristic of the BP neural network is signal passes forward and the error passes back-propagation. A typical BP-NN is a multi-layer feed forward network, which includes input layer, hidden layer and the output layer.

The BP learning process can be briefly described as follow:

(i) Forward propagation of the input signal: during the forward propagation procedure, the weight factor and the offset of the network are maintained constant. The input signal is forward propagated form the input layer, through the hidden layer, to the output layer. And the neurons state of each layer is only influent the next layer's state. If the output of the neural network does not equal the expected output, it will be transferred into the back propagation.

(ii) Back propagation of error signal: the error signal was defined as the difference between the neural network output and the expect output. The network's weights and thresholds is adjusted according to the error feedback to make the neural network real output closer to the expected one.

The BP neural network can achieve the associative memory and prediction abilities through the training. The detail of the training procedure has a lot of explanation in previous studies(Li et al., 2012). In this study, the nodes number of the input layer, hidden layer and output layer were 8, 9 and 8, respectively.

(C) Random forest

Rand Forest (RF) is a type of ensemble learning algorithm which consists of lots of individual trees, and its basic unit is the decision tree (Breiman, 2001). Random forest added an additional layer of randomness compare to the bagging method. Besides employing a different boot strap sample of the data to construct each tree, RF changes the classification pattern of the regression trees. The classical RF establishment involves two step: random sampling and completely split. Compared to the standard trees, the splitting and the selection of the root node in a random forests are done based on the information gain, where the highest information gain is the standard for the selection of the root node(Fraiwan et al., 2012). The RF is user-friendly, for there are only two parameters (n_{tree} : the

tree number in the forest; m_{try} : the variables number in the random subset), need to be set and the outcome is not sensitive to their values(Liaw and Wiener, 2001). In this study, the parameters of m_{try} has been set to 10 and n_{tree} to 500.

Appendix B: The comparison result of GA-SVM with GS-SVM, BP-NN and Random Forest.

In order to compare the performance of the GA-SVM with other machine learning methods, the Mean and Mode of indices of P (delta)/P (alpha),which is the best combinatorial features in all measures, were used as the feature to classification based on the GS-SVM, BP-NN and RF. The statistics indices of AC, SE and SP were used for performance evaluation. As shown in table S1, the results showed that the AC, SE and SP of GA-SVM are higher than other methods. Not only that but it reflects that GA-SVM has a better classification performance.

Table S1. The statistics of AC, SE and SP values of different classification with the indices of P (delta)/P (alpha) for four patterns(mean±SD)

pattern	GA-SVM			GS-SVM		
	AC(M±SD)	SE(M±SD)	SP(M±SD)	AC(M±SD)	SE(M±SD)	SP(M±SD)
I	90.64±8.84	72.73±23.31	97.98±3.82	84.29±9.48	69.79±23.14	92.91±3.92
II	81.79±5.84	50±50	85.7±3.36	80.52±5.61	50±50	85.66±2.18
III	82.14±7.99	71.59±17.45	88.24±10.16	78.36±9.77	64.09±22.54	87.20±12.81
IV	72.86±11.11	61.94±19.51	81.07±13.80	72.71±11.75	64.85±22.27	79.24±14.93
	BP-NN			RF		
	AC(M±SD)	SE(M±SD)	SP(M±SD)	AC(M±SD)	SE(M±SD)	SP(M±SD)
I	89.54±7.24	71.35±11.25	92.80±4.23	85.84±6.94	71.36±10.51	86.46±9.26
II	78.36±9.77	50±50	87.20±12.81	80.30±11.71	50±50	85.52±4.59
III	72.71±11.75	64.85±22.27	79.24±14.93	80.38±5.68	72.92±18.52	88.25±10.36

IV	91.29±8.84	62.81±22.35	98.07±4.18	71.78±8.52	57.50±15.16	80.09±10.91

Figures

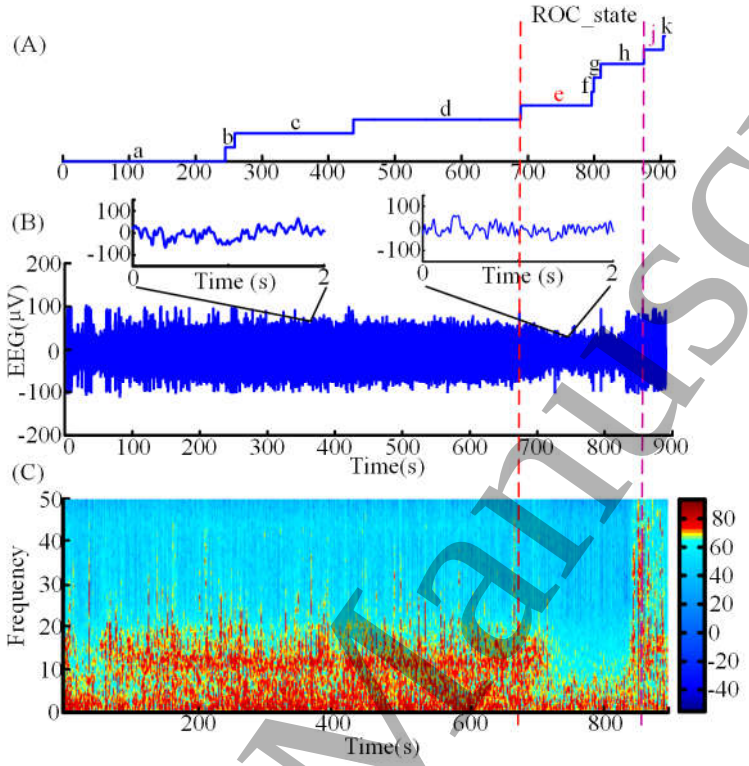

Figure 1. EEG recording from one patient of data set I for pattern I and corresponding EEG measures versus time. Start of emergence shown as a vertical red line, time of patient response as a vertical magenta. (A)Detailed anesthesia procedure of one patient. The states include: (a) awake, (b) intravenous induction, (c) tracheal intubation. (d) the surgery started (e) sevoflurane stopped. (f) propofol stopped. (g) remifentanil stopped. (h) the surgery stopped. (j) the patient regained consciousness. (k) extubation. (B) Preprocessed EEG recording. The raw EEG data were sampled at 1 kHz and then down-sampled to 100 Hz. (C) The spectrogram computed via short-time Fourier transform, using a 10s hamming window, 50% overlapping. Dark red means higher power and blue for lower power.

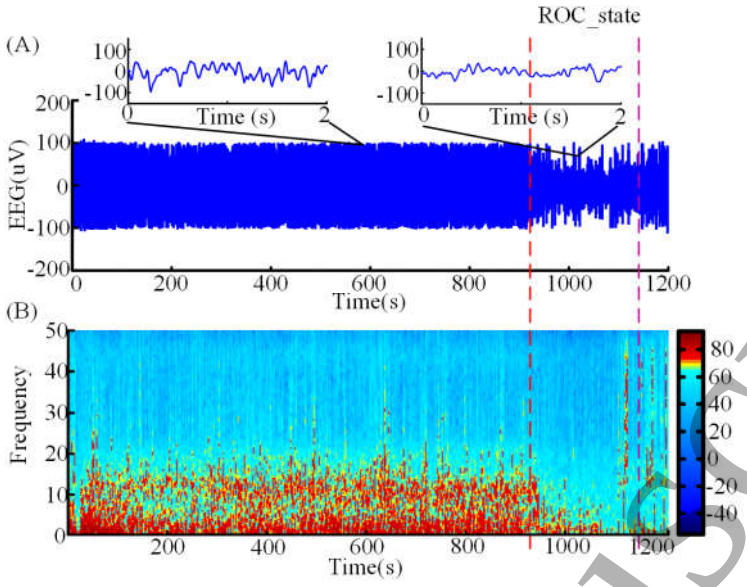

Figure 2. EEG recording from one patient of data set II for pattern II and corresponding EEG measures versus time. (A) Preprocessed EEG recording are the same as in Figure 1 (B). (B) The corresponding spectrogram of (A).

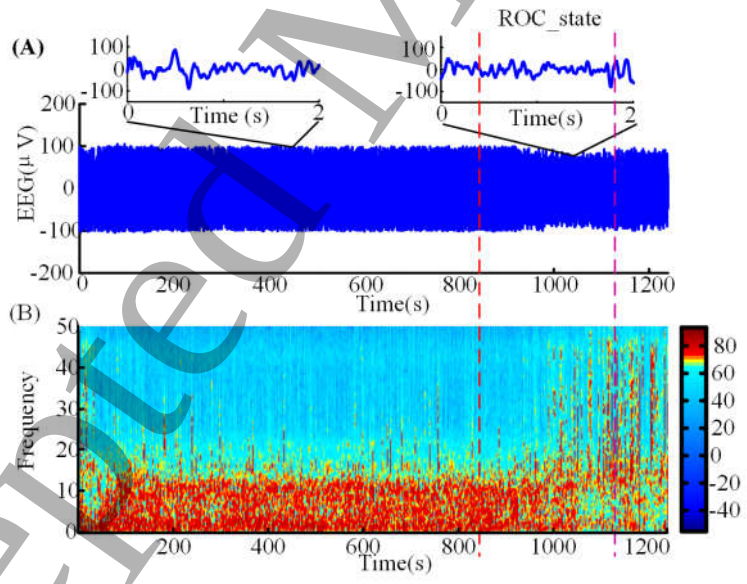

Figure 3. EEG recording from one patient of data set I for pattern III and corresponding EEG measures versus. (A) Preprocessed EEG recording are the same as in Figure 1 (B). (B) The corresponding spectrogram of (A).

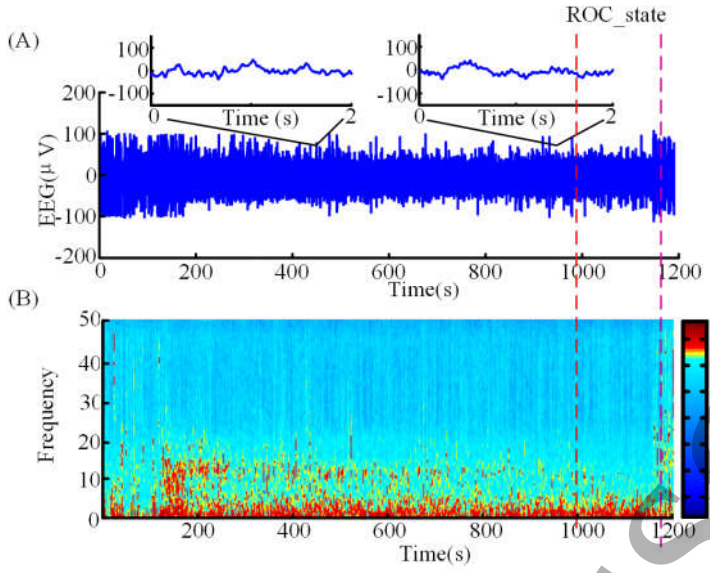

Figure 4. EEG recording from one patient of data set I for pattern IV and corresponding EEG measures versus. (A) Preprocessed EEG recording are the same as in Figure 1 (B). (B) The corresponding spectrogram of (A).

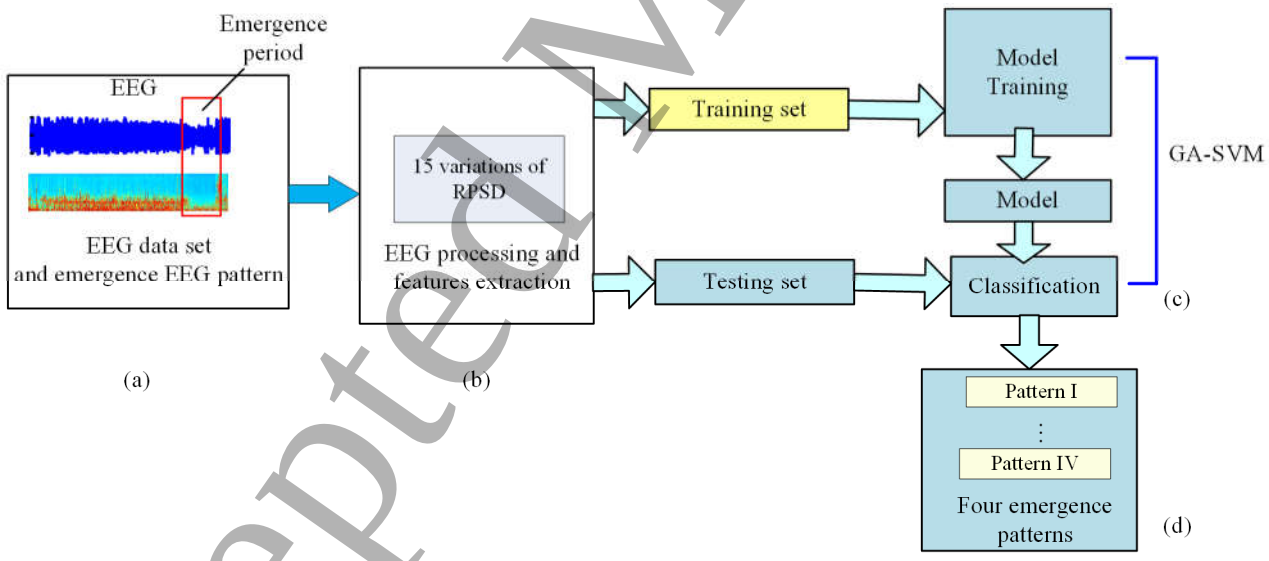

Figure 5. Schematic diagram of classification of emergence EEG patterns with GA-SVM.

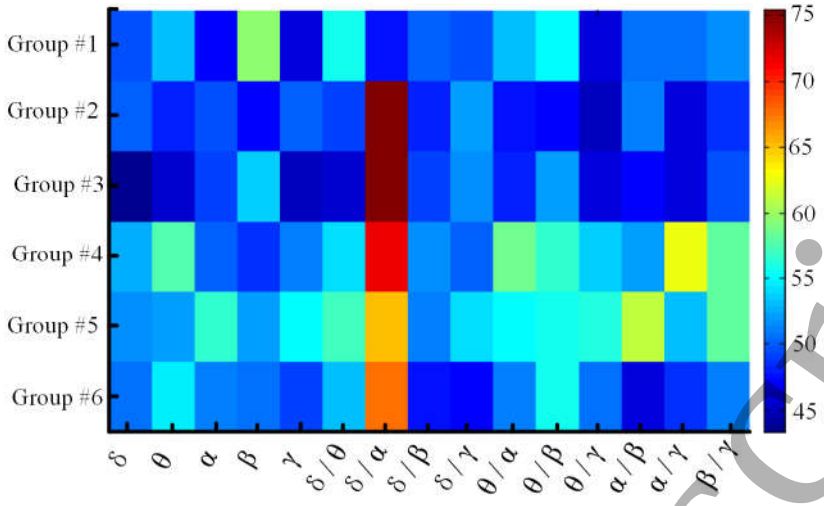

Figure 6. The cross validation accuracy of GA-SVM of 15 features with each group.

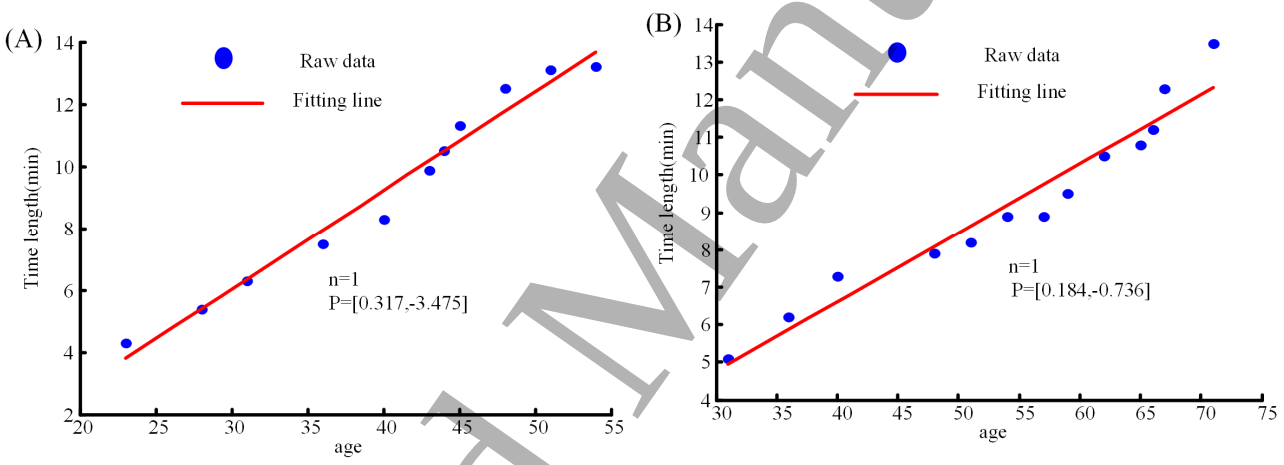

Figure 7. The trend of age and duration of recovery. The blue spot is the emergence time at that age and the red line represent the fitting line based on raw data. (A) The trend of the emergence EEG pattern I. The maximum number of fitting polynomials (n=1) and the polynomial fitting coefficients (p= [0.317,-3.475]) (B) The trend of the emergence EEG pattern III (n=1, p= [0.184,-0.736]).

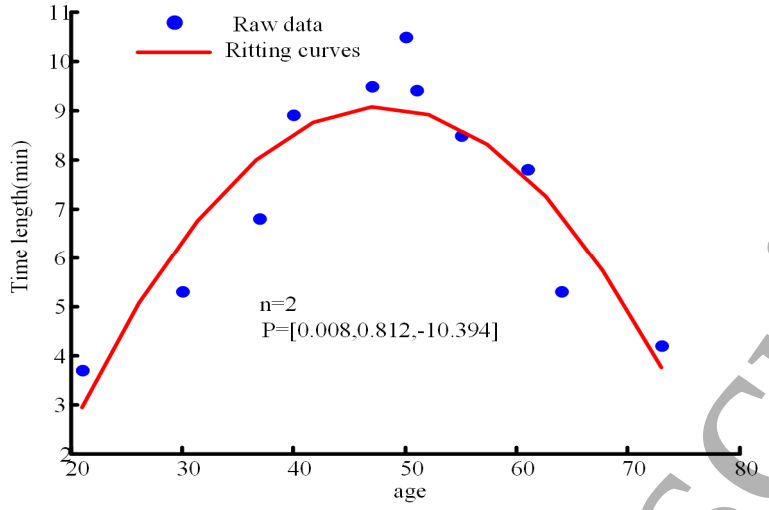

Figure 8. The trend of age and duration of recovery for the non-archetypal anesthesia (Pattern Ⅳ).The blue spot is the duration of recovery at that age and the red curves represent the fitting curves based on raw data (n=2, p= [0.008,0.812,-10394]).

Tables:

Table 1. The cross validation accuracy with different statistics indices of P (delta)/P (alpha)

Group	Statistics Indices	Accuracy of Train set	Accuracy of Test set
#1	Mean, SD	79.33±10.60	47.62±11.30
#2	Mean, Mode	87.67±5.33	75.48±10.75
#3	Median, Mode	87.22±5.26	75.23±14.34
#4	Mean, Mode, Min, Max, Median, SD	93.22±6.34	71.90±11.69
#5	Min, Mode	75.11±5.72	65.24±12.06
#6	Mean, Mode, SD	88.78±5.77	67.62±11.35

Table 2. The statistics of AC, SE and SP values of GA-SVM with the indices of P (delta)/P (alpha) for four patterns(mean±SD).

Pattern	AC(M±SD)	SE(M±SD)	SP(M±SD)
I	90.64±8.84	72.73±23.31	97.98±3.82

II	81.79±5.84	50±50	85.7±3.36
III	82.14±7.99	71.59±17.45	88.24±10.16
IV	72.86±11.11	61.94±19.51	81.07±13.80

Table 3. The statistics of patient's information with four emergence EEG patterns

	Pattern I	**Pattern II**	**Pattern III**	**Pattern IV**
Number(female)	17 (10)	4 (3)	19 (11)	12 (5)
Age(yr)	34-51	22-33	48-73	22-75
Duration of recovery(min)	4.3-24.8	6.8-15.6	9.8-24.1	2.6-17.8
EEG pattern in anesthesia maintenance stage	archetypal	archetypal	archetypal	Non-archetypal
Maintenance drugs				
Sevoflurance (% expired)	2±0.8(15)	2±0.0(4)	2±0.0(17)	2±0.0(12)
Remifentanil(ug)	589.3±150.5(16)	50±0.0(4)	506.7±212.0(15)	436.4±80.0(11)
Etomidate(mg)	13.3±8.8(6)	-	19.17±10.3(6)	12.5±5.0(6)
Propofol (mg)	88.8±49.7(14)	50±0.0(4)	122.5±81.3 (17)	81.7±53.1(9)

References

Akeju, O., Pavone, K.J., Thum, J.A., Firth, P.G., Westover, M.B., Puglia, M., Shank, E.S., Brown, E.N., and Purdon, P.L. (2015). Age-dependency of sevoflurane-induced electroencephalogram dynamics in children. *Bja British Journal of Anaesthesia* 115 Suppl 1**,** i66-i76.

Almabruk, T., Iyer, K., Tan, T., Roberts, G., and Anderson, M. (2015). An EEG coherence-based analysis approach for investigating response conflict processes in 7 and 9-year old children. *Conf Proc IEEE Eng Med Biol Soc* 2015**,** 2884-2887.

Antkowiak, B. (1999). Different actions of general anesthetics on the firing patterns of neocortical neurons mediated by the GABA(A) receptor. *Anesthesiology* 91**,** 500-511.

Bettinardi, R.G., Tort-Colet, N., Ruiz-Mejias, M., Sanchez-Vives, M.V., and Deco, G. (2015). Gradual emergence of spontaneous correlated brain activity during fading of general anesthesia in rats: Evidences from fMRI and local field potentials. *Neuroimage* 322**,** 185-198.

Bian, Z., Li, Q., Wang, L., Lu, C., Yin, S., and Li, X. (2014). Relative power and coherence of EEG series are related to amnestic mild cognitive impairment in diabetes. *Frontiers in aging neuroscience* 6(3),11.

Bojak, I., and Liley, D. (2005). Modeling the effects of anesthesia on the electroencephalogram. *Physical Review E* 71**,** 041902.

Boser, B.E., Guyon, I.M., and Vapnik, V.N. (1992). "A training algorithm for optimal margin classifiers", in: *The Workshop on Computational Learning Theory*), 144-152.

Breiman, L. (2001). Random Forests. *Machine Learning* 45**,** 5-32.

Breshears, J.D., Roland, J.L., Sharma, M., Gaona, C.M., Freudenburg, Z.V., Tempelhoff, R., Avidan, M.S., and Leuthardt, E.C. (2010). Stable and dynamic cortical electrophysiology of induction and emergence with propofol anesthesia. *Proc Natl Acad Sci U S A* 107**,** 21170-21175.

Bruhn, J., Röpcke, H., and Hoeft, A. (2000). Approximate entropy as an electroencephalographic measure of anesthetic drug effect during desflurane anesthesia. *Anesthesiology* 92**,** 715-726.

Buzsáki, G., and Draguhn, A. (2004). Neuronal oscillations in cortical networks. *science* 304**,** 1926-1929.

Chang, C.-C., and Lin, C.-J. (2011). LIBSVM: A library for support vector machines. *ACM Transactions on Intelligent Systems and Technology (TIST)* 2**,** 27.

Chen, W., Wang, Y., Cao, G., Chen, G., and Gu, Q. (2014). A random forest model based classification scheme for neonatal amplitude-integrated EEG. *BioMedical Engineering OnLine* 13**,** 1-13.

Ching, S., Cimenser, A., Purdon, P.L., Brown, E.N., and Kopell, N.J. (2010). Thalamocortical model for a propofol-induced α-rhythm associated with loss of consciousness. *Proceedings of the National Academy of Sciences* 107**,** 22665-22670.

Cortes, C., and Vapnik, V. (1995). Support Vector Network. 20**,** 273-297.

Cover, T., and Hart, P. (1967). Nearest neighbor pattern classification. *IEEE Transactions on Information Theory* 13**,** 21-27.

Fabiani, M., Gordon, B.A., Maclin, E.L., Pearson, M.A., Brumback-Peltz, C.R., Low, K.A., Mcauley, E., Sutton, B.P., Kramer, A.F., and Gratton, G. (2014). Neurovascular coupling in normal aging: A combined optical, ERP and fMRI study. *Neuroimage* 85 Pt 1**,** 592-607.

Fraiwan, L., Lweesy, K., Khasawneh, N., Wenz, H., and Dickhaus, H. (2012). Automated sleep stage identification system based on time–frequency analysis of a single EEG channel and random forest classifier. *Computer Methods & Programs in Biomedicine* 108**,** 10-19.

François, D., Rossi, F., Wertz, V., and Verleysen, M. (2007). Resampling methods for parameter-free and robust feature selection with mutual information. *Neurocomputing* 70**,** 1276-1288.

Franceschini, M.A., Radhakrishnan, H., Thakur, K., Wu, W., Ruvinskaya, S., Carp, S., and Boas, D.A. (2010). The effect of different anesthetics on neurovascular coupling. *Neuroimage* 51**,** 1367-1377.

Hight, D.F., Dadok, V.M., Szeri, A.J., García, P.S., Voss, L., and Sleigh, J.W. (2014). Emergence from general anesthesia and the sleep-manifold. *Frontiers in systems neuroscience* 8(146),146.

Hsu, C.W., and Lin, C.J. (2002). "A Comparison of Methods for Multiclass Support Vector Machines", in: *IEEE TRANS. NEURAL NETWORKS*), 415-425.

Huang, C.L., and Wang, C.J. (2006). A GA-based feature selection and parameters optimizationfor support vector machines. *Expert Systems with Applications* 31**,** 231-240.

Jameson, L.C., and Sloan, T.B. (2006). Using EEG to monitor anesthesia drug effects during surgery. *Journal of clinical monitoring and computing* 20**,** 445-472.

Jospin, M., Caminal, P., Jensen, E.W., Litvan, H., Vallverdú, M., Struys, M.M., Vereecke, H.E., and Kaplan, D.T. (2007). Detrended fluctuation analysis of EEG as a measure of depth of anesthesia. *Biomedical Engineering, IEEE Transactions on* 54**,** 840-846.

Kelz, M.B., Sun, Y., Chen, J., Meng, Q.C., Moore, J.T., Veasey, S.C., Dixon, S., Thornton, M., Funato, H., and Yanagisawa, M. (2008). An essential role for orexins in emergence from general anesthesia. *Proceedings of the*

National Academy of Sciences 105**,** 1309-1314.

Law, C., Sleigh, J., Barnard, J., and Maccoll, J. (2011). The association between intraoperative electroencephalogram-based measures and pain severity in the post-anaesthesia care unit. *Anaesthesia and intensive care* 39**,** 875.

Lee, U., Mueller, M., Noh, G.-J., Choi, B., and Mashour, G.A. (2011). Dissociable network properties of anesthetic state transitions. *Anesthesiology* 114**,** 872-881.

Li, J., Cheng, J.H., Shi, J.Y., and Huang, F. (2012). *Brief Introduction of Back Propagation (BP) Neural Network Algorithm and Its Improvement.169,553-558.*

Li, X., Cui, S., and Voss, L.J. (2008). Using Permutation Entropy to Measure the Electroencephalographic Effects of Sevoflurane. *Anesthesiology* 109**,** 448.

Liaw, A., and Wiener, M. (2001). Classification and Regression by RandomForest. *R News* 23.

Lin, C.J. (2003). A practical guide to support vector classification. http://www.csie.ntu.edu.tw/～cjlin/paper/guide.pdf, 67(5).

Mccarthy, M.M., Brown, E.N., and Kopell, N. (2008). Potential network mechanisms mediating electroencephalographic beta rhythm changes during propofol-induced paradoxical excitation. *The Journal of Neuroscience* 28**,** 13488-13504.

Mckeown, D.M. (1993). Automatic recognition of USGS land use/cover categories using statistical and neural network classifiers. *Proceedings of SPIE - The International Society for Optical Engineering* 1944**,** 185-195.

Murphy, M., Bruno, M.A., Riedner, B.A., Boveroux, P., Noirhomme, Q., Landsness, E.C., Brichant, J.F., Phillips, C., Massimini, M., Laureys, S., Tononi, G., and Boly, M. (2011). Propofol anesthesia and sleep: a high-density EEG study. *Sleep* 34**,** 283-291A.

Proakis, John, G., Manolakis, and Dimitris, G. (1992). Digital signal processing : principles, algorithms, and applications. *Digital Signal Processing：principles* 23**,** 392 - 394.

Purdon, P.L., Pavone, K.J., Akeju, O., Smith, A.C., Sampson, A.L., Lee, J., Zhou, D.W., Solt, K., and Brown, E.N. (2015). The Ageing Brain: Age-dependent changes in the electroencephalogram during propofol and sevoflurane general anaesthesia. *Bja British Journal of Anaesthesia* 115 Suppl 1**,** i46-i57.

Purdon, P.L., Pierce, E.T., Mukamel, E.A., Prerau, M.J., Walsh, J.L., Wong, K.F., Salazar-Gomez, A.F., Harrell, P.G., Sampson, A.L., Cimenser, A., Ching, S., Kopell, N.J., Tavares-Stoeckel, C., Habeeb, K., Merhar, R., and Brown, E.N. (2013a). Electroencephalogram signatures of loss and recovery of consciousness from propofol. *Proc Natl Acad Sci U S A* 110**,** E1142-1151.

Purdon, P.L., Pierce, E.T., Mukamel, E.A., Prerau, M.J., Walsh, J.L., Wong, K.F.K., Salazar-Gomez, A.F., Harrell, P.G., Sampson, A.L., and Cimenser, A. (2013b). Electroencephalogram signatures of loss and recovery of consciousness from propofol. *Proceedings of the National Academy of Sciences* 110**,** E1142-E1151.

Rampil, I.J. (1998). A primer for EEG signal processing in anesthesia. *The Journal of the American Society of Anesthesiologists* 89**,** 980-1002.

Riaz, F., Hassan, A., Rehman, S., and Niazi, I.K. (2015). EMD-Based Temporal and Spectral Features for the Classification of EEG Signals Using Supervised Learning. *IEEE Transactions on Neural Systems & Rehabilitation Engineering A Publication of the IEEE Engineering in Medicine & Biology Society* 24**,** 28-35.

Schlögl, A. (2000). *The electroencephalogram and the adaptive autoregressive model: theory and applications.* Citeseer.

Shalbaf, R., Behnam, H., Sleigh, J.W., Steyn-Ross, A., and Voss, L.J. (2013). Monitoring the depth of anesthesia using entropy features and an artificial neural network. *Journal of Neuroscience Methods* 218**,** 17-24.

Trafidło, T., Gaszyński, T., Gaszyński, W., and Nowakowska-Domagała, K. (2015). Intraoperative monitoring of cerebral NIRS oximetry leads to better postoperative cognitive performance: a pilot study. *International Journal of Surgery* 16**,** 23-30.

Viertiö‐Oja, H., Maja, V., Särkelä, M., Talja, P., Tenkanen, N., Tolvanen‐Laakso, H., Paloheimo, M., Vakkuri, A., Yli‐Hankala, A., and Meriläinen, P. (2004). Description of the Entropy™ algorithm as applied in the Datex‐Ohmeda S/5™ Entropy Module. *Acta Anaesthesiologica Scandinavica* 48**,** 154-161.

Welch, P.D. (1967). The use of fast Fourier transform for the estimation of power spectra: A method based on time averaging over short, modified periodograms. *IEEE Transactions on audio and electroacoustics* 15**,** 70-73.